NATIONAL AERONAUTICS AND SPACE ADMINISTRATION

Technical Report 32-1599

A New Broadband Square Law Detector

M. S. Reid
R. A. Gardner
C. T. Stelzried

JET PROPULSION LABORATORY
CALIFORNIA INSTITUTE OF TECHNOLOGY
PASADENA, CALIFORNIA

September 1, 1975

NATIONAL AERONAUTICS AND SPACE ADMINISTRATION

Technical Report 32-1599

A New Broadband Square Law Detector

M. S. Reid
R. A. Gardner
C. T. Stelzried

JET PROPULSION LABORATORY
CALIFORNIA INSTITUTE OF TECHNOLOGY
PASADENA, CALIFORNIA

September 1, 1975

Preface

The work described in this report was performed by the Telecommunications Division of the Jet Propulsion Laboratory.

Contents

Figures

Abstract

A new broadband constant law detector has been developed for precision power measurements, radio metric measurements, and other applications. It has a wider dynamic range and a more accurate square law response than has been available in the past. Other desirable characteristics, which are all included in a single compact unit, are high-level dc output with immunity to ground loop problems, fast response times, ability to insert known time constants, and good thermal stability. This report reviews the history of this development work and describes in detail the new detector and its performance. It also shows how the new detector can be operated in a programmable system with a ten-fold increase in accuracy, and discusses the use and performance of the detector in a noise-adding radiometer system.

A New Broadband Square Law Detector

I. Introduction

Broadband square law detectors are required for precision power measurements and a wide variety of other detector applications such as the Noise-Adding Radiometer (Ref. 1), the antenna servo boresighting system, antenna gain measurements, radio science, conical-scan tracking of spacecraft and radio sources, etc. All of the following detector characteristics are important and are desired in a single device:

(1) Wide dynamic range.

(2) Accurate square law response over the dynamic range.

(3) Good thermal stability.

(4) High-level dc output with immunity to ground loop problems.

(5) Ability to insert known time constants for radio metric applications.

(6) Fast response times compatible with computer-oriented systems.

No known commercial device has all of these characteristics in a single compact unit. Over the past 10 years, the Radio Frequency Techniques (RFT) Group at JPL has used two types of detectors in an attempt to fulfill the above requirements. Development proceeded slowly over the years along two lines: an attempt to include all of the above characteristics in a single device, and the improvement of the square law response. Recent work has culminated in a detector which has all of the above characteristics with acceptable accuracy as well as significantly improved square law response. This report reviews the history of this development work and describes in detail the new broadband square law detector and its performance alone and in various systems.

II. The Early Models

Prior to 1965, a germanium diode detector (Type 1N198 or similar) was used which was matched to a 50-Ω input. Since no dc amplification was used, this detector fulfilled conditions (5) and (6) adequately, but the other conditions were not satisfied. The square law response varied from diode to diode, and the accuracy obtained was seldom better than 10%. The detector law varied as much as 20% with temperature. Because of the low operating voltages (about 10-mV maximum output), the dynamic range was restricted to less than 20 dB. The magnitude of ground loops often exceeded the dc output signal level. Figure 1 is a circuit diagram of one of these detectors, and Fig. 2 shows its measured performance. Input power in -dBm is plotted against output voltage in mV in Fig. 2 for three different bandwidths. The response of this diode was not identical with continuous wave (CW) and noise input

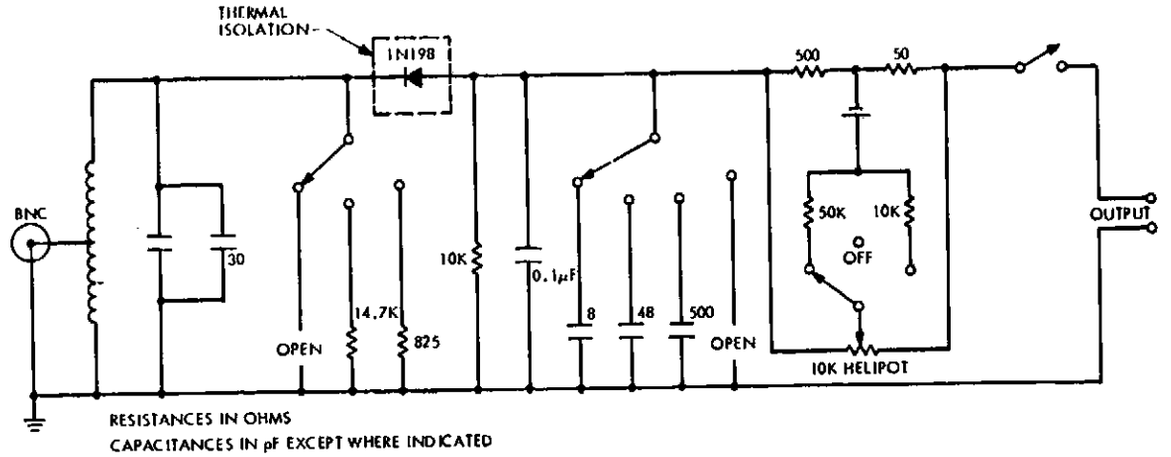

Fig. 1. Circuit diagram of early diode detector

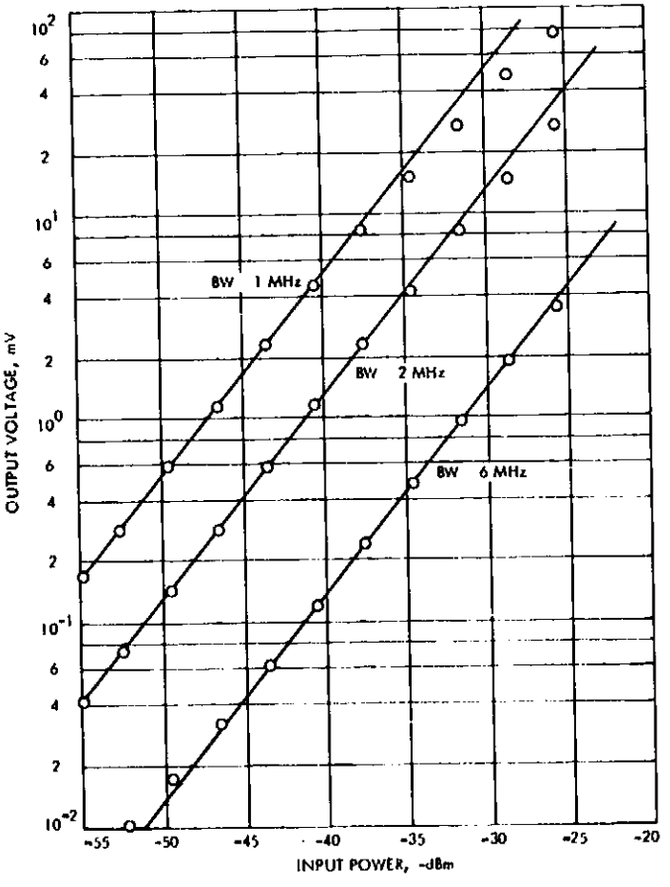

Fig. 2. Performance characteristics of an early detector

signals (Refs. 2 and 3). In order to solve this problem for the CW power calibration program (Refs. 2 and 3), a different type of detector—the power meter detector—was used.

Figure 3 is a photograph of the field model of this detector. The power meter detector consists of a commercial power meter/thermistor combination and is still in use in the Deep Space Network (DSN). Square law response is excellent, and the higher operating voltages (about 1 V) result in immunity from most ground loops. Known time constants consist of simple RC circuits. The power meter detector still has the following severe problems:

(1) Thermal drift. The square law characteristic of the power meter relies on a balance between a detection thermistor and a reference thermistor. Any environmental temperature change upsets this balance and reduces the accuracy. The device, therefore, requires frequent zero adjustments.

(2) Dynamic range. This range is limited to less than 10 dB unless scale changes are made.

(3) Response time. The response time, to 67.5% of full value, to an input level change is greater than 100 ms.

III. Recent Detector Development

When low-drift dc amplifiers became available, the construction of a diode detector with high-level output, good thermal stability, and good square law response became feasible. Several approaches were attempted before a practical device was developed. Figure 4 shows a block diagram of one of the recent detectors. The input is fed through step attenuators with an 80-dB range, a wideband IF amplifier (1 to 110 MHz) with 45-dB gain,

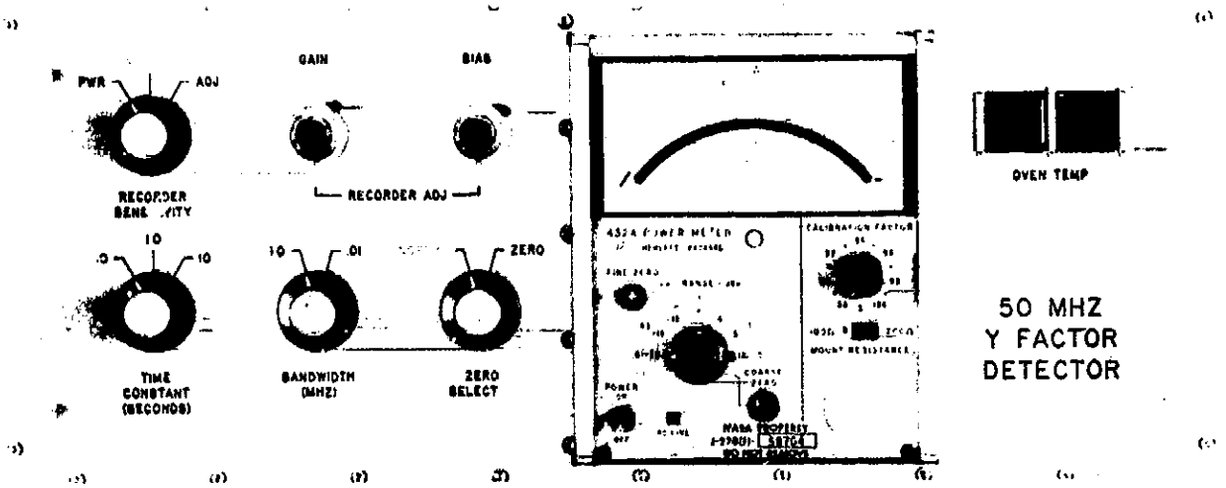

Fig. 3. Field model of power meter detector

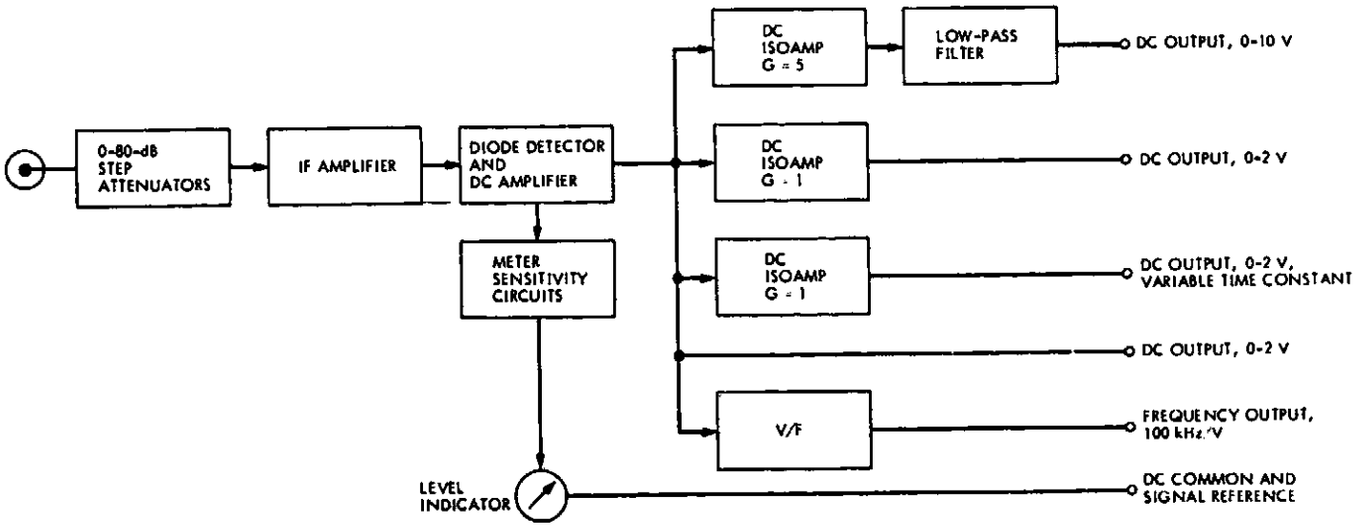

Fig. 4. Block diagram of broadband square law detector

and into a detector/amplifier unit. The dc output from this unit is available through a variety of time constant and filter circuits, a typical example of which is shown in Fig. 4. One output has a variable time constant, three outputs are fast (approximately 200 μs), and the fifth has a frequency proportional to voltage.

Figure 5 is a detailed diagram of the diode detector and dc amplifier block shown in Fig. 4. This entire circuit is enclosed in a mumetal box for radio frequency interference (RFI) and magnetic shielding. The RF portion of this circuit is RFI-shielded from the remainder, as shown. All outputs from shielded enclosures are through capacitive feed-through connectors. The inner shielded box contains the diode and an isolation transformer. Considerable effort was expended in determining the best diode type from various manufacturers for this detector application. The objective was to find the optimum compromise between sensitivity, repeatability, square law characteristics, stability, drift, etc. A type BD-3 tunnel diode was chosen. The amplifier is an Analog Devices Model 2341.

The entire circuit is packaged in a standard chassis for rack mounting. Provision is made on the front panel for

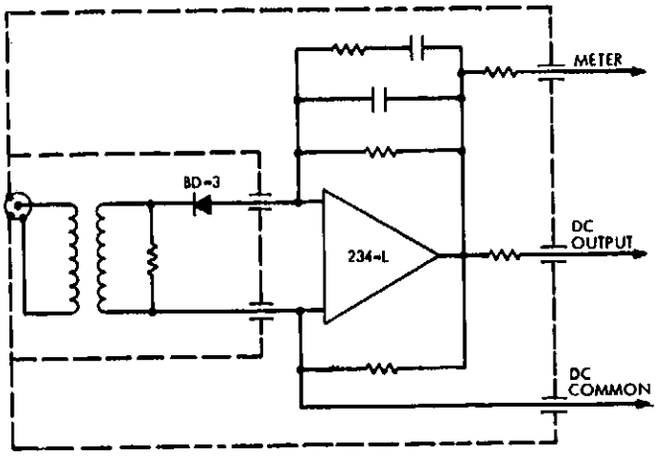

Fig. 5. Diode detector and dc amplifier

adjustment of the meter sensitivity and detector time constant as well as a dc bias offset. Figure 6 is a photograph of the engineering model.

IV. Performance

A. Dynamic Range and Square Law Response

The square law response of the detector is plotted in Fig. 7. This shows output error in dB for a 1-dB input level change as a function of output level. A high-power broadband noise source was fed through a variable attenuator and a measured 1-dB step. The output from this step switch was connected to the input of the detector, and the output was monitored in the usual way. The detector was taken over the whole range of its output voltage (0 to 2 V) by adjusting the variable attenuator. Each point on the curve was measured by switching the 1-dB step in and out. The response of a perfect detector would be a line parallel to the x-axis, which intersects the y-axis at the 1-dB point. This method of measuring the performance of the detector was developed because the characteristic of the detector was more linear than that of the equipment used in the conventional method of detector measurement. It may be seen from the figure that over the first 10 dB of detector dynamic range, the deviation from square law is 0.009 dB, whereas over the whole of the measured dynamic range (60-mV to 2-V output) of 15.6 dB, the error is 0.032 dB.

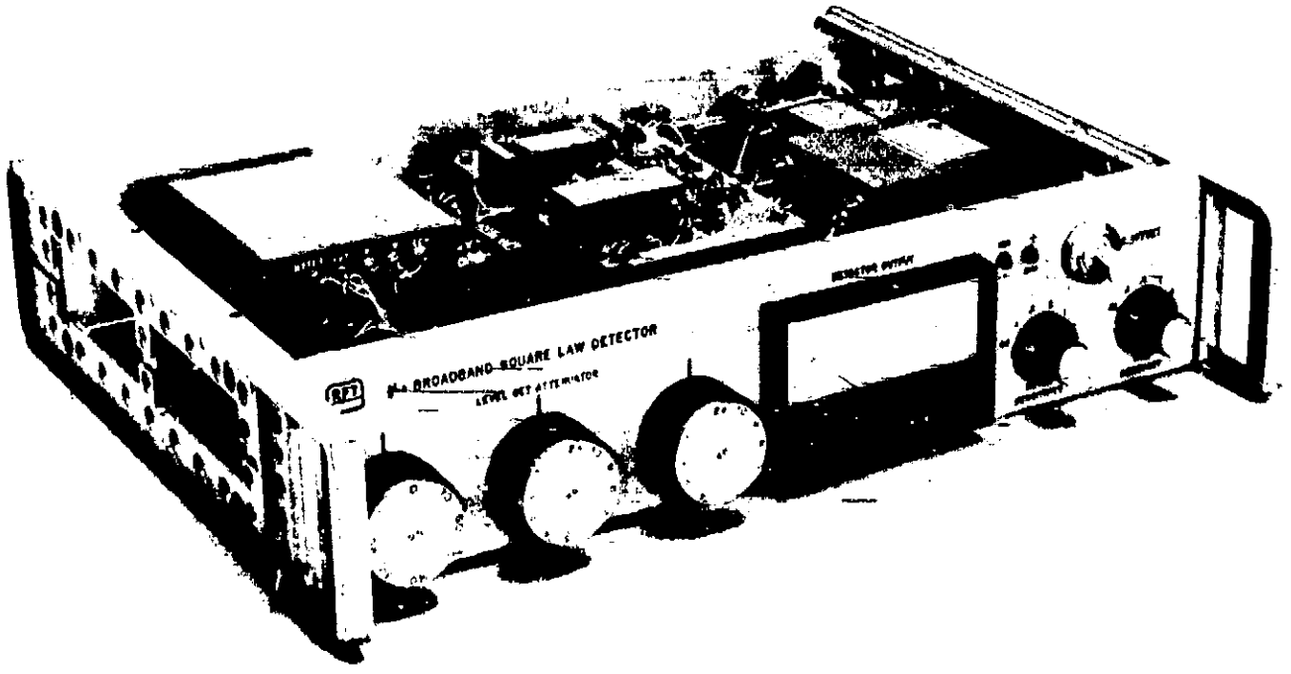

Fig. 6. Photograph of engineering model

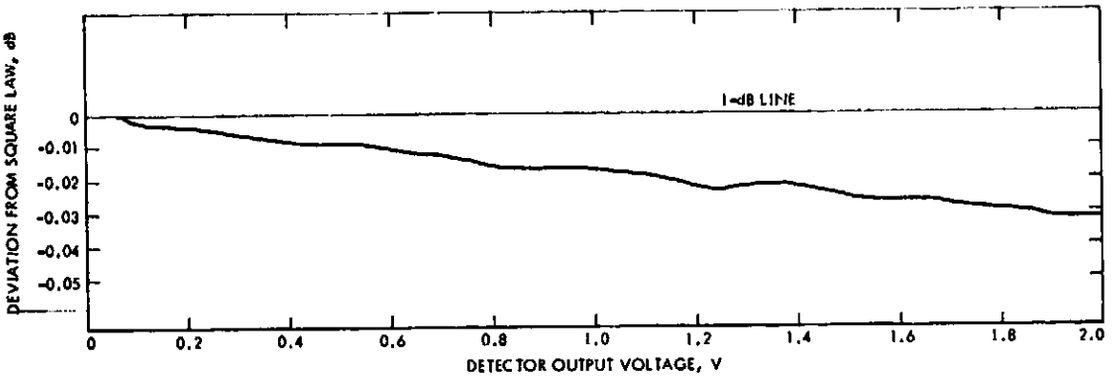

Fig. 7. Output error for 1-dB input level change as a function of output level

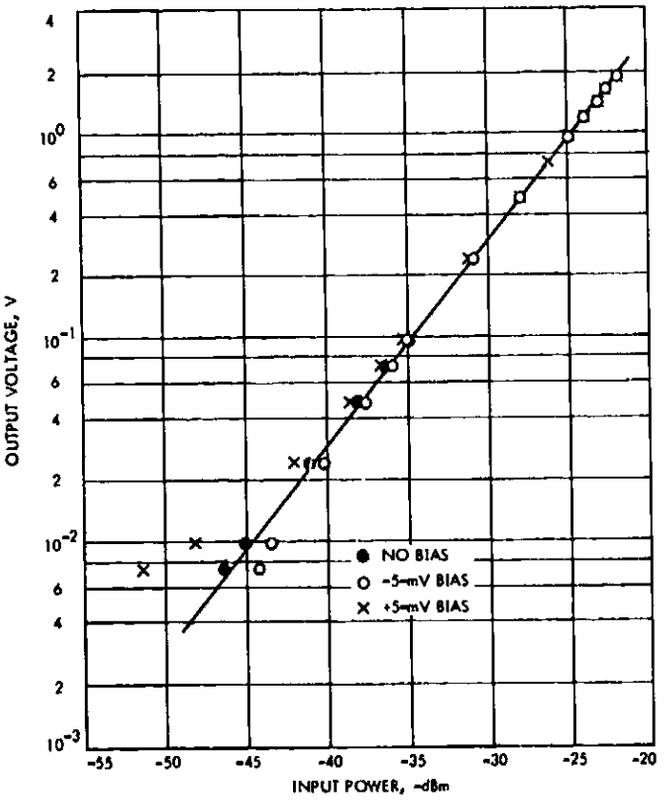

Fig. 8. Square law response for a 30-dB input range

Figure 8 shows the detector square law response for a 30-dB input range. A true square law characteristic is shown by the straight line. This conventional method of presenting the detector response does not have sufficient resolution to show the detector characteristics nor is it accurate, but it is shown here for comparison with Fig 2. It must be noted that the detector is more linear than the IF attenuator used to change the input signal level over the 30-dB range, and, therefore, Fig. 2 is more an attenuator characteristic than a detector characteristic (see Ref. 4 for details). The data of Figs. 7 and 9 were not taken in this way. Each data point in these two figures was obtained by switching the same 1-dB step in and out. Thus neither the accuracy nor the linearity of this step affects the detector output data. With the above reservations in mind, departures from square law of 0.25 dB over a 20-dB dynamic range and 0.35 dB over a 30-dB dynamic range have been taken from Fig. 8.

B. Thermal Drift

The Model 234L amplifier shown in Fig. 5 is a chopper-stabilized dc amplifier with a specified drift of 0.1 μV/°C, referred to the input. For a gain of 200, the drift, referred to the output, is 20 μV/°C. Measurements have indicated that the total drift in field installations at Goldstone is less than 0.1 mV per week.

Figure 9 shows the effect of dc offsets on the detector performance. These data were taken and plotted in the same way as the data of Fig. 7; that is, the graph is a plot of detector output error against output signal level for a 1-dB step change in input signal. It may be seen from the figure that detection performance can be improved only over a small operating range by imposing a dc offset.

The time constant networks shown in Fig. 4 are made up of resistance-capacitance circuits and are inserted by using isolation amplifiers. Since these amplifiers operate at a gain of 1 or 5, thermal drifts are insignificant.

C. Ground Loops

Since the upper range of the voltage levels in the detector are all above 1 V, most ground loops are insignificant.

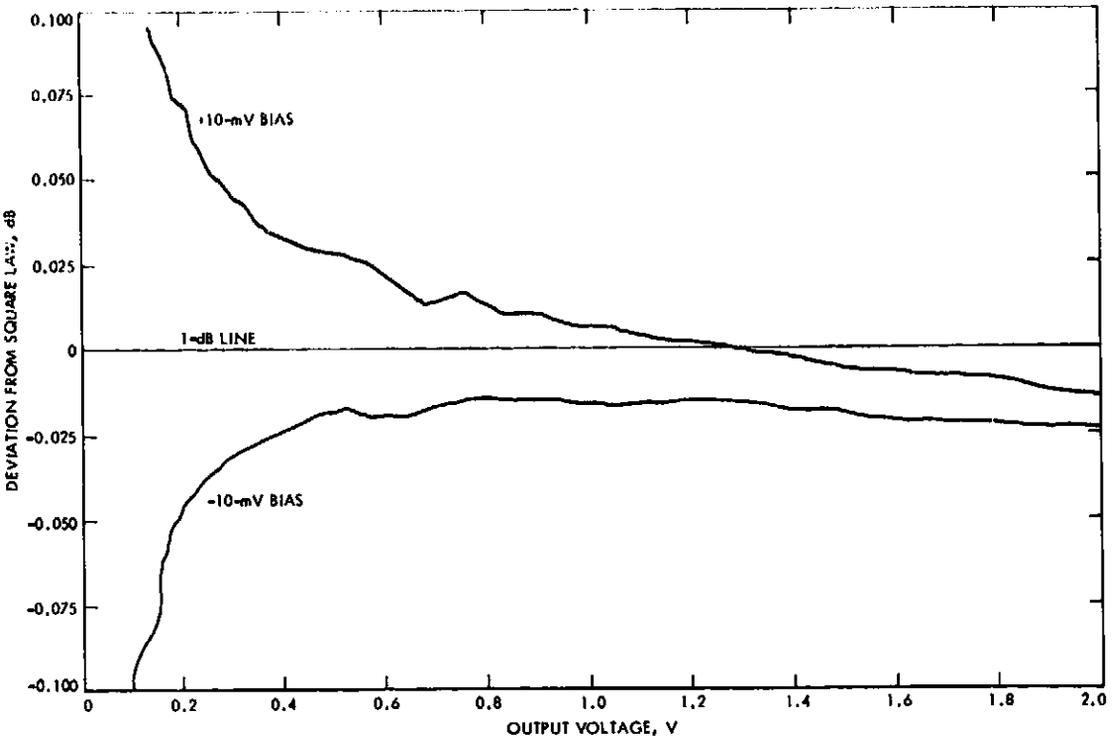

Fig. 9. Effect of dc offsets on detector response

D. Response Time

Full voltage (to 99.9% output level) rise time is less than 300 μs. Faster low-drift amplifiers are now becoming available, and it is expected that this response time will soon be lowered to less than 10 μs.

E. High-Level Output

The 0- to 10-V output shown in Fig. 4 is used for operation with an analog-to-digital converter for computer applications (Ref. 1). This output, therefore, has a low-pass filter to prevent clock feedback from the computer.

V. Thermal Stability

Figures 10 and 11 show the effect of temperature changes on the detector output. They are plots of output voltage drift as a function of detector chassis temperature.

The detector chassis was placed in an oven, and the output voltages were monitored with the input terminated. The oven temperature was changed in a series of step functions and measured at a representative point on the detector chassis. The detector temperature and outputs were recorded on a strip chart recorder.

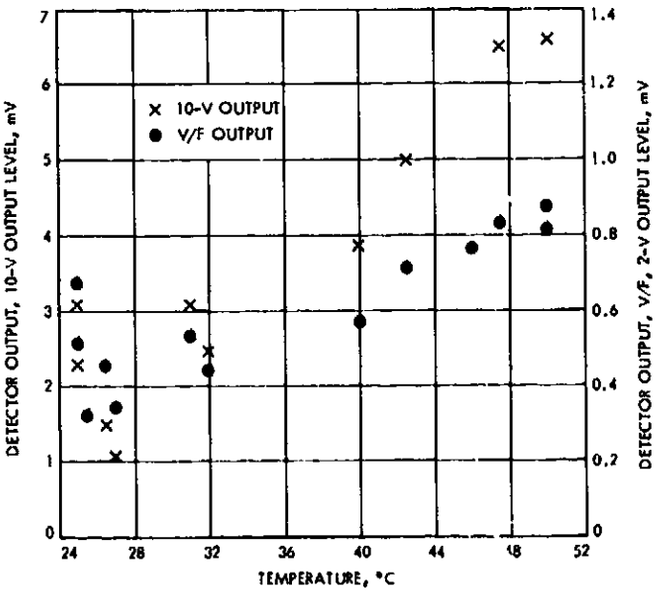

Fig. 10. Output drift as a function of temperature: typical production unit

Temperatures were allowed to stabilize for several hours before data were taken. When a step change was made in the oven temperature, the detector required some settling time before coming to a steady output voltage. For a 25°C

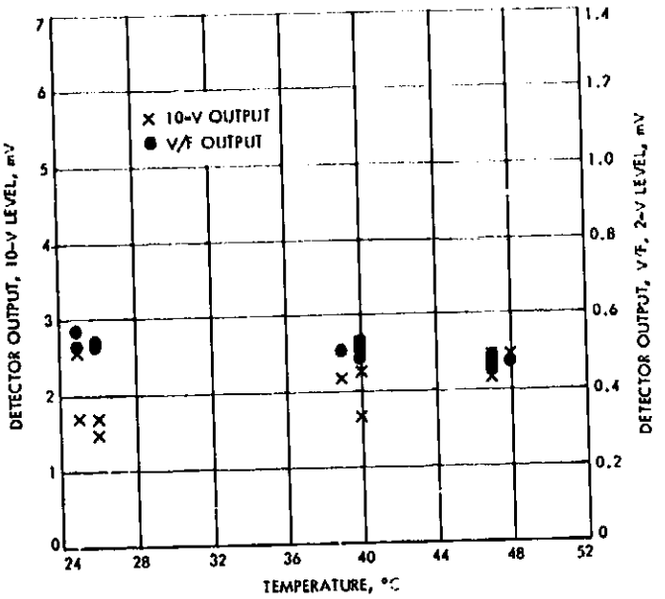

Fig. 11. Output drift as a function of temperature: selected unit

step change in temperature, the detector settling time is approximately 60 min, and typical peak transient deviations are approximately 200 μV.

Figure 10 shows voltage drift data for a typical production model of the detector, and Fig. 11 presents similar data for a selected good unit. In both figures, the crosses represent the 10-V output and the circles the 2-V V/F output. The output voltage scales for the two sets of data are, therefore, different. It must be noted that even in the production unit, the use of the amplifier to yield a 10-V output does not seriously detract from the stability of the detector.

VI. Improvement in the Accuracy of the New Broadband Detector

Conventional detectors typically have an accuracy on the order of 10%, whereas the new detector described in the preceding sections is a 3% instrument. This section discusses further development work which allows the operation of the detector in a programmable system that accounts for detector deviation from square law response. The resulting instrument has an accuracy better than 0.3%.

A. Calculator Applications and the Correction Factor

The increasing use of automatic machines for data acquisition, computation, control, and automation has led to a desire to adapt detectors and other instruments for operation with automatic digital equipment. Part of the development work described in the preceding sections (for example, fast response times and high-level dc output with immunity to ground loop problems, etc.) was directed toward detector operation in computer-oriented systems. This section shows how the new detector can be operated in a programmable system with a ten-fold increase in accuracy.

The accuracy of the detector can be increased by accounting for the detector's deviation from square law. If the output voltage of the detector is designated V, then a correction factor α may be included by multiplying the square of the output voltage by the correction factor and using this term in addition to the output voltage. Thus,

$$\text{corrected output voltage} = V + \alpha V^2 \qquad (1)$$

Nonlinearity effects, i.e., deviations from square law, can be accounted for to a large extent by using Eq. (1). With automatic digital equipment, it is easily possible to determine and to use the optimum value for the correction factor.

B. Measurements

In order to make a complete set of test measurements on a detector under controlled conditions, an automatic system was designed and set up in the laboratory. The objective of these tests was to exercise the detectors over a wide dynamic range, to investigate the effects of varying correction factors, and to determine the accuracy of a (corrected) detector with the maximum possible accuracy. The test circuit was based on the measurement system described above, where a high-power broadband noise source was fed through a variable attenuator and a measured 1-dB step. The output from this step switch was connected to the input of the detector, and the output was monitored in the usual way. The detector was taken over the whole of its output voltage range (0 to 2 V) by adjusting the variable IF attenuator. Each measurement point was determined by switching the same 1-dB step in and out. The response of a perfect detector would yield a set of points which, when plotted on a graph of deviation from square law versus output voltage, would be a line parallel to the abscissa and cutting the ordinate at the 1-dB point.

To avoid contaminating the data with human error and spending an excessive amount of time in evaluating a detector, the measurement system was automated by using a desk calculator and a coupler/controller. The automatic measurement system is shown in Fig. 12.

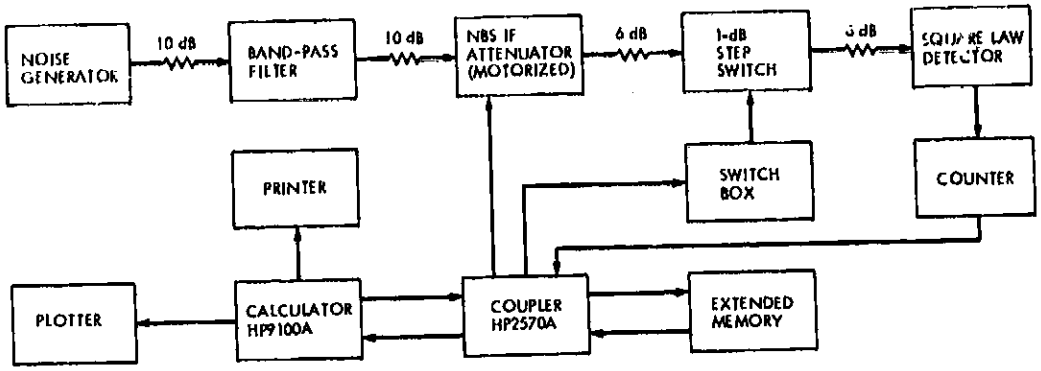

Fig. 12. Automatic measurement system

The coupler was a Hewlett-Packard 2570A Coupler/Controller, which formed an output/input interface for the Hewlett-Packard 9100A calculator. The combination of the detector's voltage-to-frequency converter and the counter gave a binary coded decimal (BCD) input, as shown in the diagram. BCD output codings were then used to switch the 1-dB step pad in and out of the circuit, and also to start the motor drive on the IF attenuator.

The sequence of measurements that were made was as follows:

(1) Adjust the IF attenuator to set the noise power level to be detected.

(2) Switch the 1-dB pad out.

(3) Measure the detected output level.

(4) Switch the 1-dB pad in.

(5) Measure the detected power level.

(6) Compute the Y factor for three values of correction factor.

(7) Reset the power level and repeat the sequence.

If V_2 is equal to the averaged voltage at the detector output with the 1-dB pad out and V_1 is equal to the averaged voltage at the detector output with the 1-dB pad in, then

$$Y = \frac{V_2 + \alpha(V_2)^2}{V_1 + \alpha(V_1)^2} \qquad (2)$$

where α is the correction factor.

The Y factor was computed and plotted in dB, as shown in Fig. 13, for three values of α. The Y factor, or difference in dB between the measurement with the pad in and out of circuit, is plotted along the ordinate, and the detector output voltage is plotted along the abscissa. The dashed curve shows the detector characteristics when the correction factor is set equal to zero. The solid curve was computed for $\alpha = 0.035$, and the dots show the curve for $\alpha = 0.037$. This figure clearly shows the improvement in linearity to be obtained when a suitable correction factor is used. It also indicates the sensitivity of the detector characteristic to small changes in the value of the correction factor.

Measurement repeatability was found to be good. If a specific pair of voltage measurements is repeated, the calculated value of the 1-dB pad repeats within ±0.002 dB.

The Y factor on the ordinate of Fig. 13 is the measured value of the nominal 1-dB pad for various values of detector output voltage. It may be seen from the figure that with $\alpha = 0.035$, the detector unit number RFT470 measured the 1-dB pad as 0.938 dB. This step pad was checked with independent measurements against a National Bureau of Standards (NBS) attenuator (Ref. 5) and found to be 0.942 ±0.001 dB. Since the NBS attenuator was calibrated with a CW signal at 50 MHz and the input in this case was broadband noise (10-MHz bandwidth) centered at 50 MHz, some of the discrepancy may be attributable to a frequency sensitivity in the NBS attenuator.

It may be seen from Fig. 13 that the detector linearity holds within 0.005 dB (i.e., 0.12%) from about 0.1 to about 2.6 V. This is a dynamic range of approximately 15 dB. The dynamic range may be extended to greater than 20 dB with a slightly reduced accuracy. On the other hand, the high-accuracy dynamic range may be extended at the low output level end to less than 0.05 V output without impairment to the accuracy by setting in the correct dc offset. The reason for an offset requirement is a small difference between the dc and the voltage-to-frequency outputs. The offset in Fig. 13 was 82 μV. Another

technique is to account for the offset by adding a constant term to Eq. (1).

Figure 14 shows the effect of varying offsets and correction factors for the same detector unit as used in Fig. 13. The correction factors are 0, 0.035, and 0.07. The solid curves were computed with a dc offset of 120 μV, the dashed curves with 59-μV offset, and the dots are the points with zero offset. It may be seen from Fig. 14 that the effect of the dc offset is to change the shape and position of the curve but only at the low-voltage end of the detector's dynamic range.

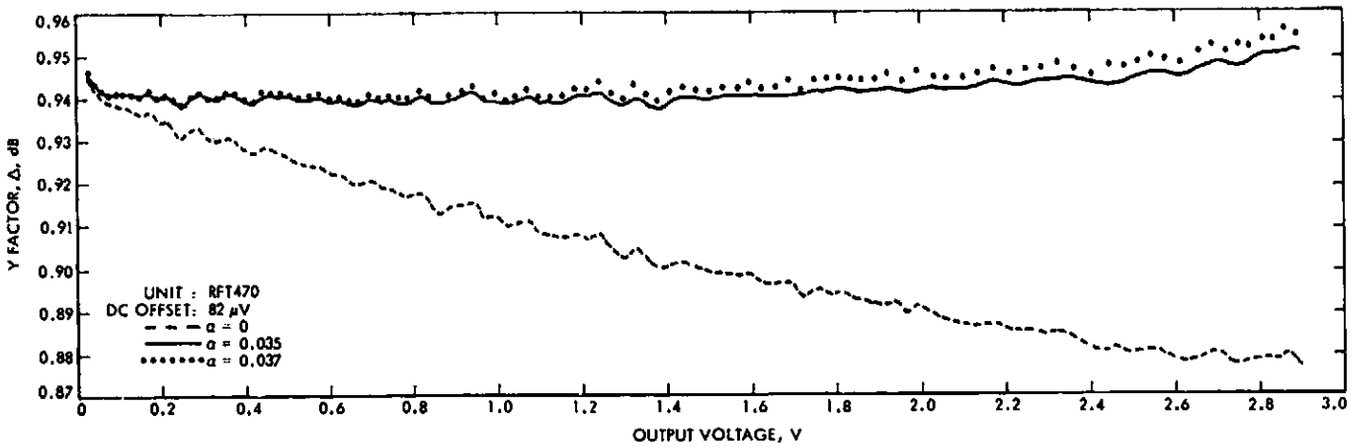

Fig. 13. Detector characteristic for three values of correction factor

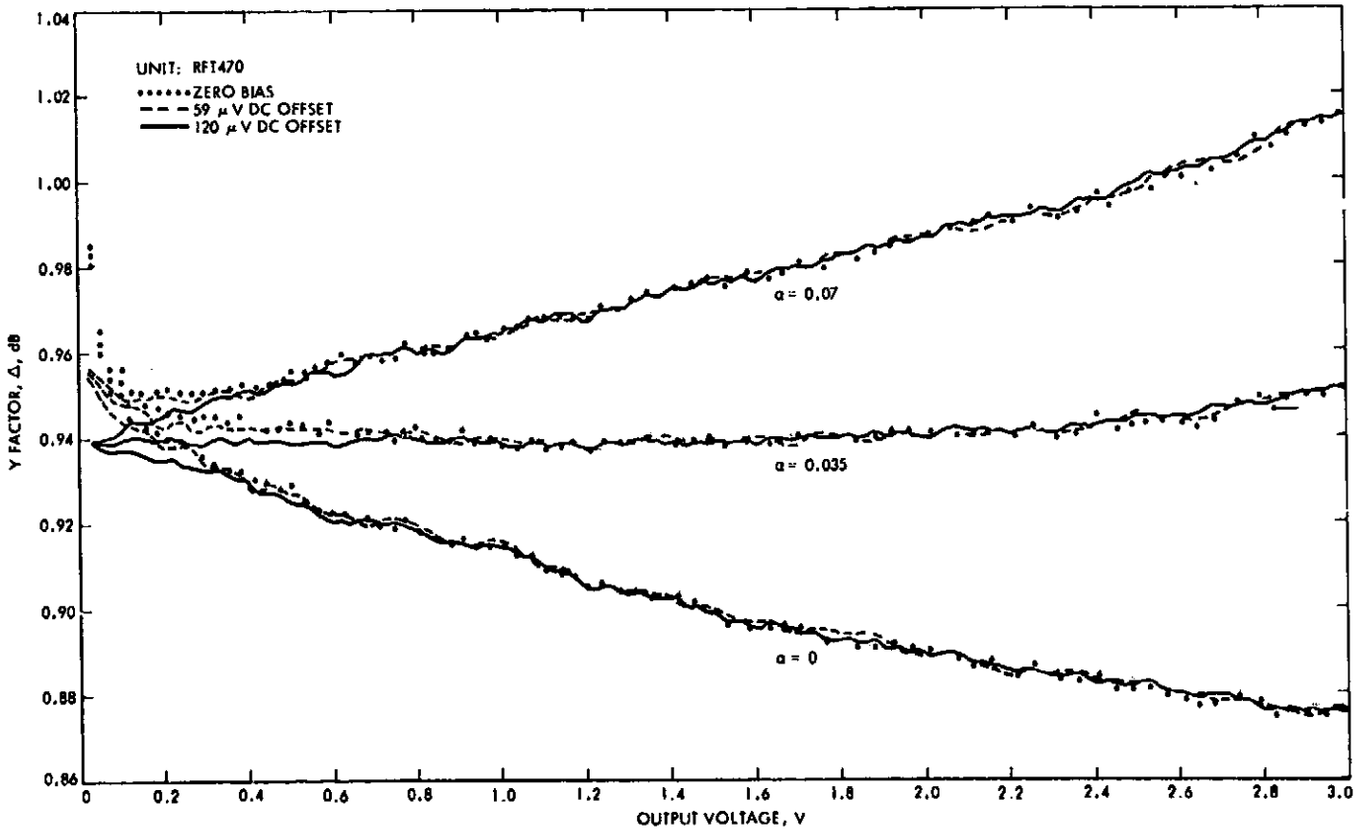

Fig. 14. Detector characteristic for various correction factors and offsets

C. Conclusions

Preceding sections discussed the development and performance of a new constant law detector with a 3% accuracy over a dynamic range of at least 15 dB. This section has shown that when this detector is used in a system with automatic digital equipment so that a large number of calculations can be performed quickly and efficiently, the accuracy can be improved by a factor of more than 10. The next section will discuss the use and performance of this detector in a noise-adding radiometer.

VII. Radio Metric Applications of the New Detector

A. The Noise-Adding Radiometer System

In a total-power radiometer, the output system noise temperature T_{op} is given by

$$T_{op} = GKV \tag{3}$$

where G is the system gain, V is the voltage output from the square law detector, and K is a scaling constant. In the total-power radiometer system, gain changes cannot be distinguished from real antenna temperature changes. In order to desensitize a receiving system from gain changes, a noise-adding radiometer may be used. If a known and constant amount of noise is added to the system and used as a reference, then it is possible to obtain a ratio of output powers (Y factors) with the noise reference source on and off. Thus,

$$Y = \frac{G(T_{op} + T_N)}{G(T_{op})} \tag{4}$$

and

$$T_{op} = \frac{T_N}{Y - 1} \tag{5}$$

where T_N is the equivalent noise temperature of the noise reference. It has been found that a temperature-stabilized solid-state noise diode is sufficiently stable for noise-adding radiometer applications. If the Y factors are measured at a rate much faster than the gain changes in the receiving system, the effect of gain fluctuations is cancelled.

A noise-adding radiometer system has been designed and constructed at DSS 13 for operation with the 26-m antenna. The maser preamplifier operates in a closed-cycle refrigerator (CCR). The CCR compressor cycles at a 1.2-Hz rate which is determined by the ac power-line frequency. Since the maser gain fluctuates at this rate, it is desirable to switch T_N at a rate greater than 8 Hz. It is also important to choose a rate that will not cohere with the 1.2-Hz CCR rate. The resolution of the radiometer, for a switching rate of 8 Hz (which corresponds to a measurement time of 0.125 s), is given by

$$\Delta T = \frac{2T_{op}\,(1 + T_{op}/T_N)}{(\tau B)^{1/2}}$$

$$= \frac{2(20)(1 + 20/117)}{(40 \times 10^{-3} \times 10 \times 10^{6})^{1/2}} \approx 0.1\text{K} \tag{6}$$

where τ is the measurement time for one Y factor and B the system bandwidth. Thus, the resolution is 0.1K for a single measurement of T_{op} from one Y factor for the DSS 13 radiometer. This resolution is improved, by averaging a number of individual measurements, by the factor $1/(N)^{1/2}$. This results in a radiometer system with a measurement resolution on the order of a milli-Kelvin.

Figure 15 shows a block diagram of the DSS 13 NAR system. In the figure, ND is the solid-state noise diode in an oven. Any detector departure from true square law has two effects: (1) measurement inaccuracy and (2) susceptibility to gain fluctuation. Thus, all measurements are corrected by a factor α, as described in the preceding sections, so that the measurement Y factor is given by

$$Y = \frac{T_{op} + T_N}{T_{op}} = \frac{V_2 + \alpha(V_2)^2}{V_1 + \alpha(V_1)^2} \tag{7}$$

where V_1 and V_2 are the detector output voltages with the noise diode off and on, respectively. The IF bandwidth at the input to the detector is 5 MHz. The frequency output from the detector is fed to the computing counter.

The computing counter is a Model H.P. 5360A, and the computer counter programmer is a Model H.P. 6376A. These two units comprise a small computing system with input/output capability, which is capable of executing 200 program steps with an average execution time of 15 μs per step. It is also capable of accepting input data in BCD form, reading an externally generated frequency, and performing various external functions by means of TTL-type signal levels. In addition, six-digit constants are available in thumbwheel form for use in the program. The

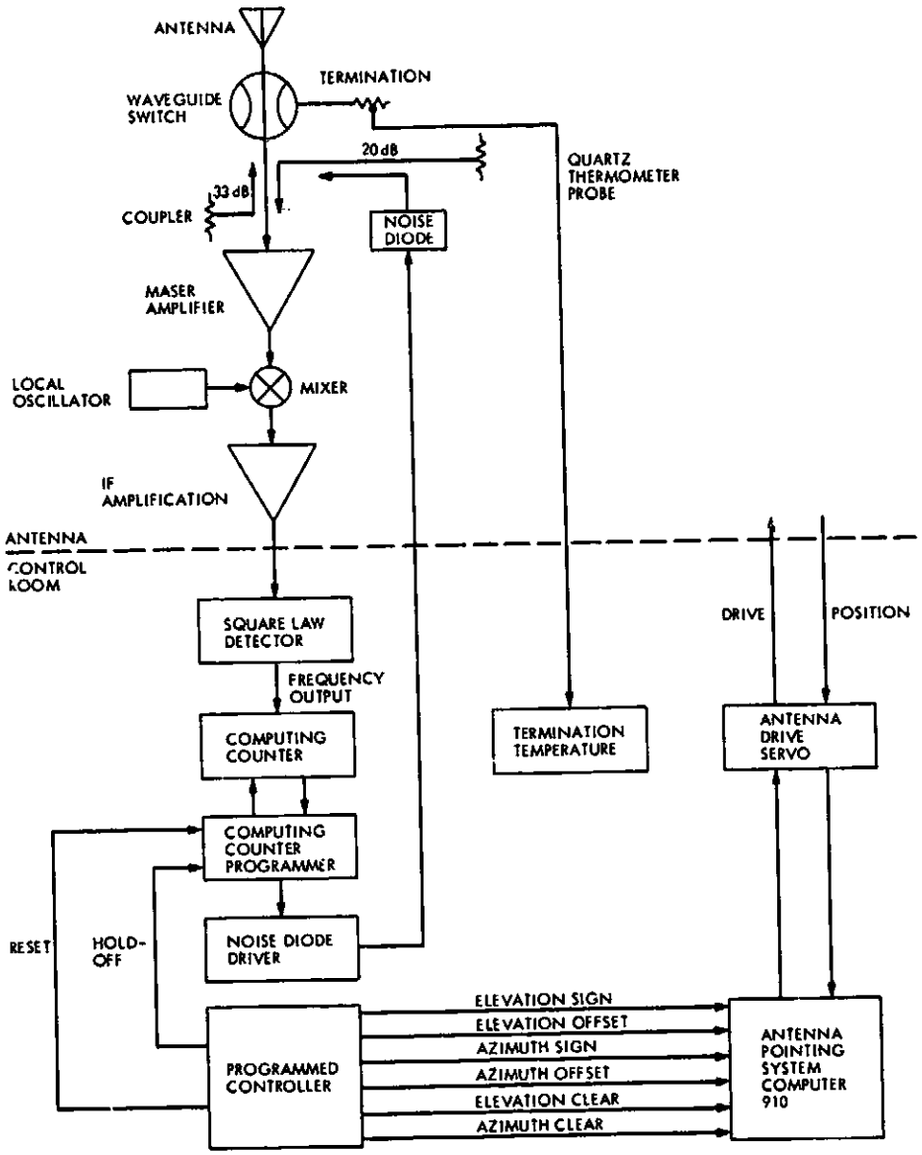

Fig. 15. Block diagram of DSS 13 NAR system

programmer commands the noise source driver whieh turns the noise diode on and off.

The programmed controller, Model 601, commands the computing counter and interfaces with the station XDS 910 computer, as shown in Fig. 15. The programmed controller commands the 910 with azimuth and elevation offset functions, and the 910 drives the antenna servo in the usual way. The programmed controller is described in detail in Ref. 6.

B. Method of Operating the NAR System

The detector correction factor α is first measured and then set on the thumbwheels of the programmer as a system constant for the duration of the NAR observing period. To determine the correct value for the correction factor, the α thumbwheels are first set to zero, the waveguide switch is switched to the ambient load, the NAR is run, and the detected output level is set to 1.8 V, with the noise diode on. The ambient load is connected to the maser input to ensure a constant system temperature during the measurement of α. There is the possibility of

radio sources passing into or out of the antenna beam if the maser is connected to the horn at this time. The IF input level to the detector is then reduced by 10 dB, and a new system temperature is computed. If the system temperature at the lower gain setting is lower than the system temperature at the higher gain, a greater value for α is required. The correct value for α is found experimentally by determining that value of α which produces the same value of T_{op} for both gain settings.

The second system constant that must be determined is the correct value for T_N. When this is found, it is entered in the second set of thumbwheels and held constant for the duration of the experiment. With the ambient termination on the maser input, the system temperature is given by

$$T_{op} = T_P + T_M + T_F \tag{8}$$

where

T_P = physical temperature of the ambient termination measured with a quartz thermometer probe.

T_M = equivalent input noise temperature of the maser.

T_F = equivalent input noise temperature of the followup receiver.

If the maser is turned on and off, a Y factor ratio Y_{OO} is measured. This ratio is given by

$$Y_{OO} = \frac{T_P + T_M + T_F}{T_P + T_F} \tag{9}$$

With a knowledge of T_M and T_P and a measurement of Y_{OO}, T_F can be calculated. The system temperature with the ambient termination on the maser input is then known. The T_N thumbwheel is adjusted until the NAR computes the correct system temperature. The maser input is then switched to the antenna, and the NAR computes the system temperature on the antenna.

The third thumbwheel constant to be determined is N, the number of measurements which are averaged to yield the output system temperature T_{op}. Since measurement certainty is given by

$$\Delta T_{RMS} = \frac{\Delta T}{(N)^{1/2}} \tag{10}$$

where ΔT is the measurement resolution as stated above, a value for N may be chosen that will produce the desired radiometer resolution. If the antenna is moving in elevation during the measurement, N should be kept sufficiently small so that the real change in antenna temperature does not exceed the desired ΔT_{RMS}.

The noise diode is enclosed in a constant-temperature (50°C) oven. Repeated measurements over an extended period of time have shown that the value of T_N varies approximately ±2% in a 24-h period in S-band systems. This fluctuation in the value of T_N seems to follow ambient temperature variations. Recent laboratory work indicates that the coupling factor of the waveguide coupler used to inject T_N varies as a function of ambient temperature. Further work is in progress on this problem.

A number of NAR programs are available for various engineering and radio science applications.

VIII. Conclusions

A new broadband constant law detector has been developed for a variety of detector applications. The detector has all of the following characteristics included in a single, compact device:

(1) Wide dynamic range.

(2) Accurate square law response over the dynamic range.

(3) Good thermal stability.

(4) High-level dc output with immunity to ground loop problems.

(5) Ability to insert known time constants for radio metric applications.

(6) Fast response times compatible with computer-oriented systems.

Each of these characteristics has been discussed in the report.

Conventional detectors have an accuracy on the order of 10%, whereas the new detector is a 3% instrument over a wider dynamic range. The report has also discussed further development work which allows the operation of this detector in a programmable system that accounts for detector deviation from square law response to yield an instrument whose accuracy is better than 0.3%. Finally, the report has described the use of the detector for radio metric applications in a noise-adding radiometer system and thus demonstrated the compatibility of the detector with computers.

An operational model of the new detector has been produced and is now implemented at all 26-m and 64-m antennas in the Deep Space Network (Ref. 7).

References

1. Batelaan, P. D., Goldstein, R. M., and Stelzried, C. T., "A Noise-Adding Radiometer for Use in the DSN," in *The Deep Space Network*, Space Programs Summary 37-65, Vol. II, pp. 66–69. Jet Propulsion Laboratory, Pasadena, Calif., Sept. 30, 1970.

2. Stelzried, C. T., and Reid, M. S., "Precision Power Measurements of Spacecraft CW Signal Level with Microwave Noise Standards," *IEEE Trans. Instrumentation and Measurement*, Vol. IM-15, No. 4, pp. 318–324, Dec. 1966.

3. Stelzried, C. T., Reid, M. S., and Nixon, D. L., *Precision Power Measurements of Spacecraft CW Signal With Microwave Noise Standards*, Technical Report 32-1066. Jet Propulsion Laboratory, Pasadena, Calif., Feb. 15, 1968.

4. Reid, M. S., Gardner, R. A., and Stelzried, C. T., "The Development of a New Broadband Square Law Detector," in *The Deep Space Network Progress Report*, Technical Report 32-1526, Vol. XVI, pp. 78–86. Jet Propulsion Laboratory, Pasadena, Calif., Aug. 15, 1973.

5. Stelzried, C. T., Seidel, B. L., Eranco, M. M., and Acheson, D., "Improved RF Calibration Techniques: Commercial Precision IF Attenuator Evaluation," in *The Deep Space Network Progress Report*, Technical Report 32-1526, Vol. XII, pp. 74–82. Jet Propulsion Laboratory, Pasadena, Calif., Dec. 15, 1972.

6. Parham, O. B., "The Design and Performance of a Programmed Controller," in *The Deep Space Network Progress Report*, Technical Report 32-1526, Vol. XIX, pp. 105–109. Jet Propulsion Laboratory, Pasadena, Calif., Feb. 15, 1974.

7. *Broadband Square Law Detector Assembly*, Jet Propulsion Laboratory DSN Technical Manual, TM509438, Dec. 1974 (JPL internal document).

NASA -- JPL — Coml., L.A., Calif.